

# Long-term persistence of oil from the *Exxon Valdez* spill in two-layer beaches

Hailong Li<sup>\*</sup> and Michel C. Boufadel<sup>†</sup>

**Oil spilled from the tanker *Exxon Valdez* in 1989 (refs 1, 2) persists in the subsurface of gravel beaches in Prince William Sound, Alaska. The contamination includes considerable amounts of chemicals that are harmful to the local fauna<sup>3</sup>. However, remediation of the beaches was stopped in 1992, because it was assumed that the disappearance rate of oil was large enough to ensure a complete removal of oil within a few years. Here we present field data and numerical simulations of a two-layered beach with a small freshwater recharge in the contaminated area, where a high-permeability upper layer is underlain by a low-permeability lower layer. We find that the upper layer temporarily stored the oil, while it slowly and continuously filled the lower layer wherever the water table dropped below the interface of the two layers, as a result of low freshwater recharge from the land. Once the oil entered the lower layer, it became entrapped by capillary forces and persisted there in nearly anoxic conditions that are a result of the tidal hydraulics in the two-layered beaches. We suggest that similar dynamics could operate on tidal gravel beaches around the world, which are particularly common in mid- and high-latitude regions<sup>4,5</sup>, with implications for locating spilled oil and for its biological remediation.**

Patches of subsurface oil from the 1989 *Exxon Valdez* spill persist in gravel beaches in Prince William Sound<sup>1,2,6</sup>. The oil varies in weathering degree from slightly to heavily weathered, and contains polycyclic aromatic hydrocarbons known to be toxic to organisms<sup>3</sup>. To investigate the factors causing the subsurface oil persistence, we conducted field studies during the summers of 2007, 2008 and 2009 on six beaches (Fig. 1a), and used physically based numerical models to interpret the results.

Our report focuses on the data from the beach EL-056C (Fig. 1) on Eleanor Island at the coordinates 147° 34' 17.42" W, 60° 33' 45.57" N. It is a single pocket beach with an along-shore width of ~40 m and an across-shore length of ~50 m. Despite its own specificity, the beach provides, in some terms, a clear illustration of the processes occurring in other gravel beaches. In particular, there was great contrast between the heavily oiled right transect and the completely clean left transect notwithstanding the small distance between both transects (Fig. 1b), and subsurface oil samples from locations R4, R5 and R6 were only slightly weathered.

To quantify the beach groundwater dynamics, we conducted a tracer study using lithium as a conservative tracer, and measured the salinity and tracer concentration at various depths using multiport wells placed at 12 locations (L1–L6 and R1–R6 in Fig. 1b). We also measured pore-water temperature and pressure at well bottoms of 11 of the 12 locations. The latter was calibrated against the measured barometric pressure and seawater density to estimate the water table. The observations started from 10:10, 28 July 2007 (the initial time  $t = 0$  for this paper) and had a maximum duration of

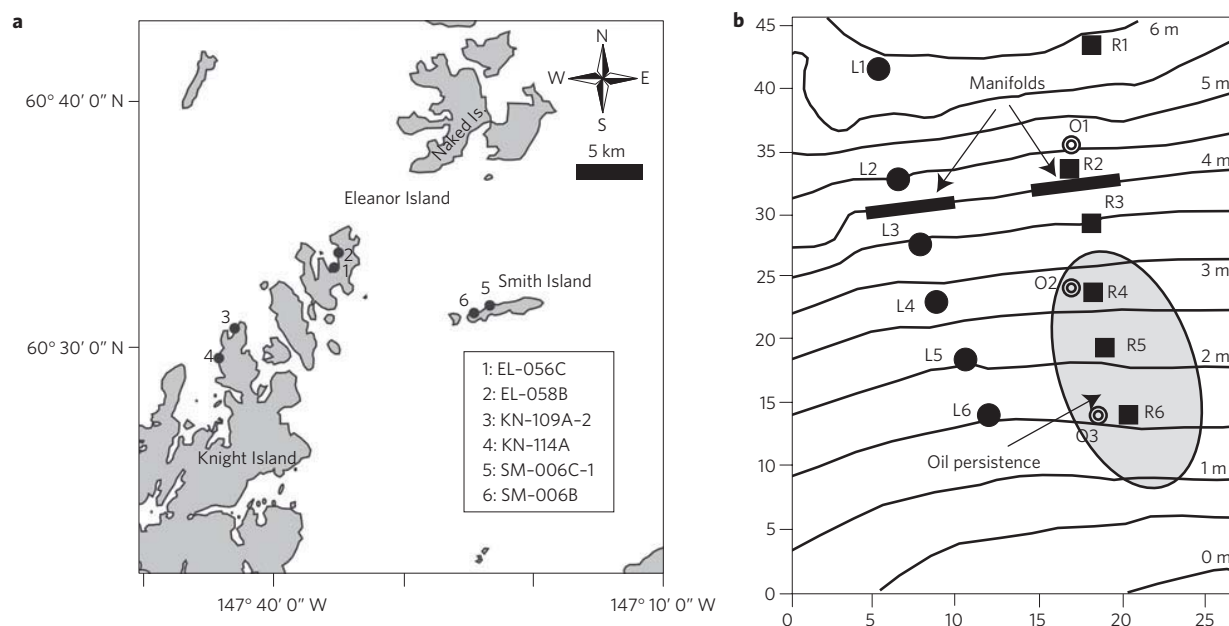
108 h at most locations. Details of the measurements are given in the Methods section.

Figure 2a shows that when the observed water table at R2 fell below the beach surface, it continued falling at the same speed as the tide until reaching a depth where its speed became abruptly much slower than that of the falling tide. The same behaviour was observed at other wells in the intertidal zones of this beach (Supplementary Fig. S3) and the other five beaches we studied (Fig. 1a). These features suggest that these beaches have two layers of different hydraulic properties: an upper layer the permeability of which is so high that the water table within it falls as fast as the falling tide, and a lower layer the permeability of which is so low that the water table does not drop much within it. Such a two-layered structure model was supported by qualitative descriptions of the beaches in mid- and high-latitude regions including Prince William Sound<sup>2,4</sup>. To our knowledge, this is the first time that the effect of the two-layered structure on tidal beach hydraulics has been quantified, as existing studies<sup>7–9</sup> did not report the abrupt change in the falling speed of the water table noted in Fig. 2a.

Figure 2b shows that, during low tides, the salinity decreased to almost zero at L4, whereas it remained larger than  $15 \text{ g l}^{-1}$  at R4 (Fig. 1b). Salinities observed at other pairs of wells in the intertidal zone (L2 versus R2, L3 versus R3, L5 versus R5, and L6 versus R6) had similar differences (Supplementary Fig. S4). These findings indicate that freshwater recharge into the left transect was much larger than that into the right transect. Supplementary Fig. S3 shows that, during low tides, all of the observed and simulated water tables were higher than the two layers' interface at the left transect and lower than it at the right transect. Thus, freshwater recharge into the left transect sustained a high water table during low tides. In contrast, the freshwater recharge into the right transect was comparatively small, allowing the water table there to drop into the lower layer. Therefore, oil from the *Exxon Valdez* floating on the water table when it arrived at the beach did not enter the lower layer of the left transect, but it entered that of the right transect, and persisted there because it was entrapped by capillarity as a result of the low permeability of that layer.

As the landward water table did not vary between transects (constant at 5.15 m at R1 and L1), the magnitude of the freshwater recharge was due to the difference in beach stratigraphy; at the left transect, the upper layer was deep (thick) and reached below the landward water table (Supplementary Table S1, Supplementary Fig. S1). Therefore, freshwater flow into the beach was large at the left transect because of the high permeability of the upper layer. On the right transect, the upper layer was shallow and above the landward water table, which was thus in contact with the low-permeability lower layer, resulting in a small freshwater flow into the beach.

Department of Civil and Environmental Engineering, Temple University, 1947 N. 12th Street, Philadelphia, Pennsylvania 19122, USA. <sup>\*</sup>Present address: School of Water Resources and Environmental Science, China University of Geosciences-Beijing, Beijing 100083, China. <sup>†</sup>e-mail: boufadel@temple.edu.



**Figure 1 | Layout and information about the study.** **a**, Locations of the beaches studied in 2007–2008 (filled circles). **b**, Topographic contours of the beach and locations of the 12 observation wells, of the two lithium tracer application manifolds and the three dissolved oxygen measurement wells (O1, O2 and O3 indicated by double-circle symbols). The lowest low tide mark during measurement was assigned as the elevation datum (0.0 m). Well names begin with 'L' for the left transect and with 'R' for the right. All dimensions are in metres. Heavy subsurface oil residues were found at locations R4, R5 and R6.

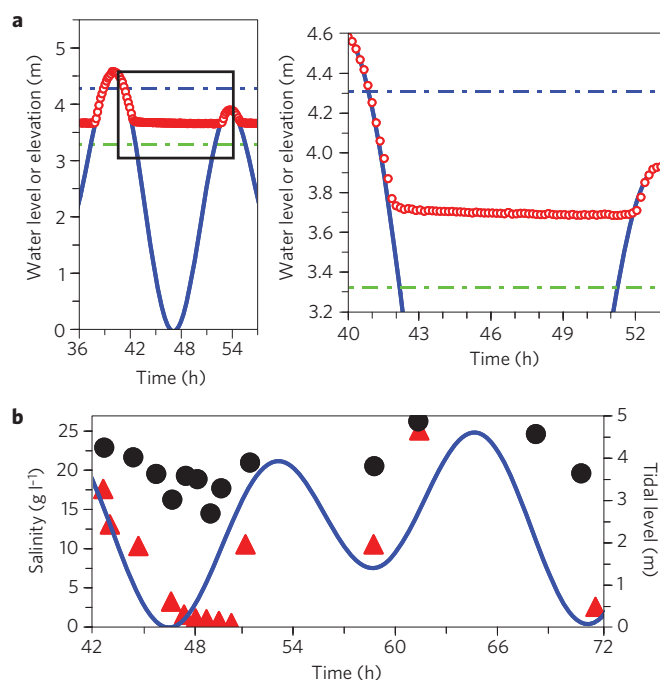


**Figure 2 | Typical observations.** **a**, Observed water table at R2 (**a**) and salinities at L4 and R4 (**b**). The red open circles represent the water table. The tidal level (solid blue line), and elevations of the beach surface (blue dashed line) and of the pressure transducer (green dashed line) installed at R2 are also shown. The water table fell from the surface (4.31 m) as quickly as the tide to ~3.7 m where it became almost constant. Note the decrease in salinity during the first low tide at L4 (depth 0.57 m) of the left transect (red triangles) in comparison with R4 (depth 0.54 m) of the right transect (black dots).

The two-layered structure increased the possibility for the oil to penetrate into the lower layer; the rapid fall of the water table with the falling tide in the high-permeability upper layer allowed oil

stranded on the beach surface to penetrate easily the upper layer's interstices, sheltering it from continued weathering and keeping its original low viscosity and high fluidity. In this regard, the upper layer acted as an oil reservoir for the slow, continuous filling of the lower layer whenever/wherever the water table dropped below the two layers' interface. If the high-permeability upper layer did not exist, the oil on the beach surface would have penetrated only into a very thin skin of beach owing to the quick weathering and loss of its high fluidity. Thus, subsurface oil persistence would not have occurred.

Our numerical simulations of density-coupled groundwater flow and salt transport using the two-layered structure (Supplementary Table S1 and Supplementary Fig. S1) closely reproduced the observed water table (Supplementary Fig. S3), salinity (Supplementary Fig. S4) and lithium concentration (not shown here) in both transects. The difference between the simulated and observed water tables was in most cases less than 0.05 m, which is excellent considering a tidal range of 4.6 m. The model parameter values are summarized in Supplementary Table S2. In particular, the hydraulic conductivity,  $K$ , was  $10^{-2} \text{ m s}^{-1}$  and  $10^{-5} \text{ m s}^{-1}$  for the upper and lower layers, respectively.

Laboratory grain-size distribution and porosity were obtained for sediment samples from the two layers. The results were used to predict the  $K$  value using the Kozeny–Carman equation<sup>10</sup>. The average  $K$  values were  $0.018 \text{ m s}^{-1}$  and  $0.0035 \text{ m s}^{-1}$  for the upper and lower layers, respectively (Supplementary Tables S3 and S4, Supplementary Fig. S5). The large difference between the laboratory-measured and model-calibrated  $K$  values of the lower layer is because the sediments of the lower layer were tightly packed within the beach and became loose on extraction before analysis in the laboratory. The difference is much smaller for the upper layer because the sediments of that layer in the field were subjected to a small overburden pressure, and were mobilized by waves and possibly by bioturbation by foragers.

Figure 3 reports time series of simulated pore-water velocity at 0.1 m below the layers' interface (that is, in the lower layer) at three locations. One notes that water flow was outward from the lower layer for most of the time. Our modelling results indicate that

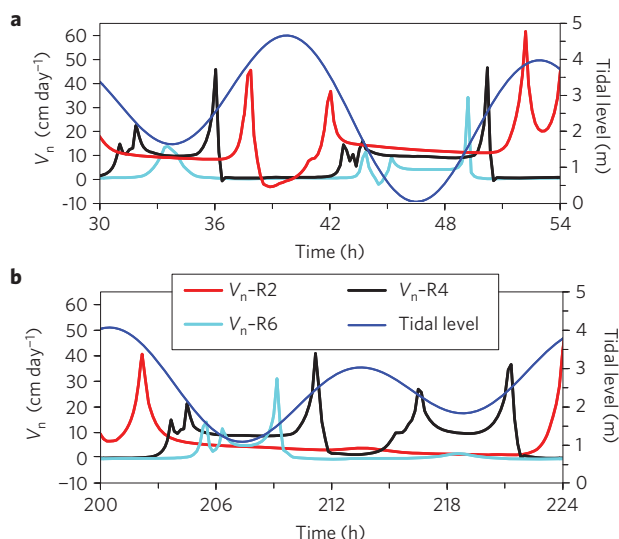


**Figure 3 | Changes of simulated pore-water normal velocities with time at three different locations in the right transect.** **a**, During a spring tidal cycle. **b**, During a neap tidal cycle. The normal velocity is defined as the velocity perpendicular to the interface of the two layers and was computed at 10 cm below that interface. Subsurface oil was located at R4 and R6. The three locations were chosen at R2, R4 and R6 (Fig. 1) at 0.1 m below the two layers' interface, where subsurface oil is located.

the bulk of the water in the lower layer comes from the landward side (Fig. 4), and more than six months would be required for it to travel from R1 ( $x = 0$  m) to R6 ( $x = 30$  m), as estimated from the average pore velocity in Fig. 4. This would cause the pore water to lose its dissolved oxygen as it satisfies the biochemical oxygen demand of naturally occurring organic matter in the sediments<sup>11</sup>. Thus, water arriving at the oil in the mid-intertidal region was depleted of oxygen. In addition, the outward flow from the lower layer opposes molecular diffusion that would bring oxygen from the sea water into the lower layer. This was confirmed by measurements of the dissolved oxygen concentration of the pore water in the lower layer along the oiled transect during summer 2009 (see the Methods section and Supplementary Fig. S6). The measured dissolved oxygen concentration was  $4.25 \pm 0.3$ ,  $1.19 \pm 0.3$  and  $1.03 \pm 0.3$  mg l<sup>-1</sup> at pits O1, O2 and O3 (Fig. 1), respectively. These values indicate depletion of oxygen in the middle intertidal zone (O2 and O3) of the beach, an observation not reported previously. The sampled water contained an unknown contribution from the upper layer (as a result of the pit effect discussed in the Methods section) where the dissolved oxygen content was measured to be larger than 8.0 mg l<sup>-1</sup>, and one concludes that the dissolved oxygen concentration in the lower layer is lower than the low values reported above. Therefore, anoxic or near-anoxic conditions exist in the lower layer, causing the persistence of the *Exxon Valdez* oil spill, similar to what was found with other spills<sup>12,13</sup> and in contrast to the argument of ref. 14. Removal of oil from the beach by clay-oil flocculation<sup>15</sup> is not likely to occur as a result of the lower permeability of the lower layer. Data from this beach are typical of the six beaches that we studied in the sense that they indicate a two-layer stratigraphy with oil persisting at locations of low freshwater recharge.

Gravel and mixed sand/gravel beaches are widely distributed around the shorelines of the world, especially in mid- and high-latitude regions<sup>4,5</sup>. For example, they account for ~33% of the shoreline of the UK<sup>16</sup> and ~48% of the paraglacial leading edge coast of southern Alaska<sup>5</sup>. All such beaches most likely have the two-layered structure because the fine sand and granule-sized particles brought to the beach surface by storms, runoff and so on

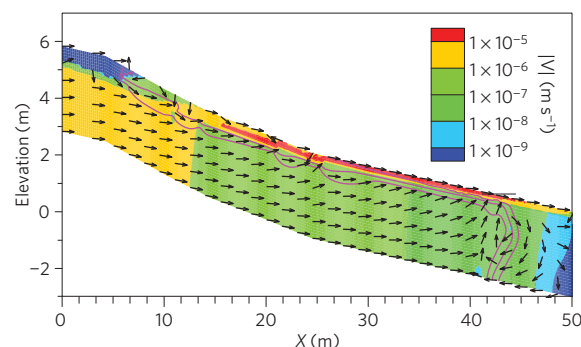


**Figure 4 | Average pore-water velocity and salinity in the right transect.**

The averages were calculated over a spring-neap tidal cycle. The magnitude of the average pore-water velocity is reported as banded coloured contours because of its wide value range. Vectors with uniform length were used to indicate the velocity direction alone. The three solid pink curves are contours of the pore-water/seawater salinity ratio (simulated pore-water salinity divided by seawater salinity) averaged over a spring-neap tidal cycle. They are for 0.1, 0.5 and 0.9, and should be read from lower-left to upper-right.

will be winnowed vertically and laterally (seawards) out of the upper layer in the intertidal zone by the tidal and wave actions and animal activities, whereby forming an open, high-permeability covering layer. The smaller grains fill and accumulate downwards, forming a low-permeability lower layer. The two-layered structure is relatively stable because the gravels of the upper layer are less sensitive to transport actions of tides, waves and small storms owing to the high threshold of the sediment entrainment velocity<sup>4,17,18</sup>. Oil tends to be more persistent on gravel beaches than on sand beaches<sup>2,4,5</sup>. Examples include the 1970 *Arrow* (Nova Scotia, Canada), the 1974 *Metula* (Strait of Magellan, Chile) and the 1978 *Amoco Cadiz* (Brittany, France) oil spills<sup>4,5</sup>. As global warming is melting the ice cover and exposing the Arctic to oil exploitation and shipping<sup>19,20</sup> through sea routes such as the Northwest Passage<sup>21</sup>, the risk of oil spills on gravel beaches in high-latitude regions will be increased. Effective protection and clean-up of spilled oil in the Arctic will be challenging, considering the difficult environmental conditions and a general lack of responder expertise in cold-water oil-spill response. Thus, our findings are of direct application for the susceptibility of beaches worldwide to long-term oil contamination, and provide guidelines for remediating oil-polluted beaches.

## Methods

**Tracer study.** Tracer studies were conducted on the left and right transects in parallel using a solution of 3.6 g of lithium nitrate per litre of sea water. Along each transect, 1,050 l tracer solution was applied through small holes (diameter 2 mm) uniformly distributed along the whole length of the manifold placed on the beach surface (Fig. 1b). The tracer was applied during the falling tide, started at 03:54, 30 July 2007 and lasted for 2 h and 6 min. The flow rate through each unit length of the 5-m-long manifold was  $100 \pm 3.6$  l h<sup>-1</sup> m<sup>-1</sup>. During tracer injection, no ponding was observed on the beach surface. Tracer concentration sampling began immediately after the tracer injection.

**Field measurements.** At each location of 12 wells along the two transects, a pit was excavated to depths of 0.66–1.17 m, and a whole-length-slotted polyvinyl chloride pipe and a multiport sampling well were installed vertically (Supplementary Fig. S2). A pressure transducer (MiniDiver, Data Logger-DL501, Schlumberger) was placed at the bottom of the polyvinyl chloride pipe to record the water pressure every 10 min. The readings of the pressure transducer were calibrated against the barometric pressure monitored by an air-pressure sensor (BaroLogger, DL-500, Schlumberger) during the same period. No rain or strong winds happened during the experiment.

The stainless-steel multiport sampling well contained four ports labelled A, B, C and D from the bottom up, which were covered with a fine stainless-steel screen to prevent blockage by fine sediments. The distance between any two adjacent ports is 23 cm. Each port was connected to a stainless-steel tube that extended to

the top of the well where it was connected by means of Tygon tubing to a luer lock three-way valve (Supplementary Fig. S2d). Water samples (approximately 100 ml) were collected with 50 ml luer lock syringes from the multiport sampling wells and placed in 125 ml polyethylene bottles. The samples were acidified by  $\text{H}_2\text{SO}_4$  (98%) and shipped to the laboratory at Temple University for chemical analysis of chlorine and lithium concentration. The chlorine concentration was transformed into salinity using the well-known chlorine–salinity ratio of 19.4:35 (ref. 22) for each of the total 361 samples. The average salinity in 19 samples collected from the sea water adjacent to the beach was  $26.45 \text{ g l}^{-1}$ .

The dissolved oxygen concentration was measured during low tide. Pore water was pumped from the Sampling Box installed in the lower layer into a 150 ml glass beaker through a flexible tube (Masterflex, inner diameter 0.95 cm, Cole Palmer) using a peristaltic pump (Masterflex, L/S 12VDC, Cole Palmer; Supplementary Fig. S6). The pumping lasted about 10 min with a pumping rate of  $0.5 \text{ l min}^{-1}$  to ensure complete removal of the existing pore water in the Sampling Box. Then a dissolved oxygen probe (YSI 85, accuracy  $\pm 0.3 \text{ mg l}^{-1}$ ) was inserted into the beaker that was full of pore water, and stirred gently as required by the manufacturer until the dissolved oxygen reading was stabilized and recorded.

**Numerical simulations.** Two-dimensional variable density and saturation simulations were carried out using the finite-element model MARUN (refs 23–25); MARUN is able to simulate two components, one is salinity and another could be nutrients<sup>26</sup> or a tracer as in this letter. The variable pore-water saturation, relative permeability and capillary pressure were described by the *van Genuchten*<sup>27</sup> model. The simulated domains for the left and right transects as well as the boundary conditions are shown in Supplementary Fig. S1. The mesh resolution was  $\sim 0.10 \text{ m}$ .

The tracer injection was simulated by specified water flow rate and concentrations of salt and tracer during the injection at the boundary node on the beach surface closest to the manifold. An analytical expression including five tidal harmonics was used to represent the tidal level (Supplementary Fig. S7). It can represent 95% of the tidal potential<sup>28</sup>, which is of sufficient accuracy for our purpose.

In each pit dug for installation of the observation wells, the original compacted, less permeable material in the lower layer was replaced by the loosened, mixed materials from the surface and lower layers. This significantly enhanced the permeability in the pit. Therefore, in calibrating the model parameters, the pit was represented by a zone of the same permeability as the upper layer, which is 0.3–0.6 m wide in the  $x$  direction, and as deep as the buried tip of the sampling well (Supplementary Table S1, Supplementary Fig. S2c). After the model parameters were identified, simulations without pits and tracer injection were conducted to investigate the effects of groundwater flow on the distribution of dissolved oxygen in the lower layer.

The simulation started from a hydrostatic initial condition at low tide with a sharp freshwater–seawater interface approximated by the well-known Ghyben–Herzberg approximation<sup>29</sup> and was run dozens of spring-neap tidal cycles to obtain a quasi-steady-state numerical solution. The variable time step was controlled by a Courant number less than 0.90. The mesh was made fine enough to meet the strict criterion for the grid Péclet number not to exceed 2.0 (ref. 30).

Received 13 March 2009; accepted 4 December 2009;  
published online 17 January 2010

## References

- Neff, J. M., Owens, E. H., Stoker, S. W. & McCormick, D. M. in *Exxon Valdez Oil Spill—Fate and Effects in Alaskan Waters* (eds Wells, P. G., Butler, J. N. & Hughes, J. S.) 312–346 (ASTM: American Society for Testing and Materials, 1995).
- Hayes, M. O. & Michel, J. Factors determining the long-term persistence of Exxon Valdez oil in gravel beaches. *Mar. Pollut. Bull.* **38**, 92–101 (1999).
- Peterson, C. H. *et al.* Long-term ecosystem response to the Exxon Valdez oil spill. *Science* **302**, 2082–2086 (2003).
- Owens, E. H., Taylor, E. & Humphrey, B. The persistence and character of stranded oil on coarse-sediment beaches. *Mar. Pollut. Bull.* **56**, 14–26 (2008).
- Hayes, M. O., Michel, J. & Betenbaugh, D. V. Intermittently exposed, coarse-grained gravel beaches. *J. Coast. Res.* doi:10.2112/2108-1071.2111 (2009).
- Short, J. W. *et al.* Estimate of oil persisting on the beaches of Prince William Sound 12 years after the Exxon Valdez oil spill. *Environ. Sci. Technol.* **38**, 19–25 (2004).

- Nielsen, P. Tidal dynamics of the water table in beaches. *Water Resour. Res.* **26**, 2127–2134 (1990).
- Gibbes, B., Robinson, C., Li, L., Lockington, D. & Li, H. L. Tidally driven pore water exchange within offshore intertidal sandbanks: Part II numerical simulations. *Estuar. Coast. Shelf Sci.* **79**, 121–132 (2008).
- Robinson, M. A. & Gallagher, D. I. A model of ground water discharge from an unconfined coastal aquifer. *Ground Water* **37**, 80–87 (1999).
- Carrier, W. D. Goodbye, Hazen; Hello, Kozeny–Carman. *J. Geotech. Geoenviron. Eng.* **129**, 1054–1056 (2003).
- Slomp, C. & Van Capellen, P. Nutrient inputs to the coastal ocean through submarine groundwater discharge: Controls and potential impact. *J. Hydrol.* **295**, 64–86 (2004).
- Burns, K. A. *et al.* The Galeta Oil Spill. II. Unexpected persistence of oil trapped in mangrove sediments. *Estuar. Coast. Shelf Sci.* **38**, 349–364 (1994).
- Reddy, C. M. *et al.* The West Falmouth oil spill after thirty years: The persistence of petroleum hydrocarbons in marsh sediments. *Environ. Sci. Technol.* **36**, 4754–4760 (2002).
- Short, J. W. *et al.* Slightly weathered Exxon Valdez oil persists in gulf of Alaska beach sediments after 16 years. *Environ. Sci. Technol.* **41**, 1245–1250 (2007).
- Bragg, J. R. & Yang, S. H. in *Exxon Valdez Oil Spill—Fate and Effects in Alaskan Waters* (eds Wells, P. G., Butler, J. N. & Hughes, J. S.) 178–214 (ASTM: American Society for Testing and Materials, 1995).
- Van Wellen, E., Chadwick, A. J. & Mason, T. A review and assessment of longshore sediment transport equations for coarse-grained beaches. *Coast. Eng.* **40**, 243–275 (2000).
- Isla, F. I. Overpassing and armouring phenomena on gravel beaches. *Mar. Geol.* **110**, 369–376 (1993).
- Trenhaile, A. S. *Coastal Dynamics and Landforms* (Oxford Univ. Press, 1997).
- Doyle, R. Melting at the top. *Sci. Am.* **292**, 31–31 (2005).
- Doggett, T. Global Warming Exposes Arctic to Oil, Gas Drilling (2004); available at <http://www.energybulletin.net/node/3072>, access date: 27 September 2009.
- Cressey, D. Arctic melt opens Northwest passage. *Nature* **449**, 267–267 (2007).
- Duxbury, A. B. & Duxbury, A. C. *Fundamentals of Oceanography* 4th edn (McGraw-Hill, 2001).
- Boufadel, M. C., Suidan, M. T., Rauch, C. H., Venosa, A. D. & Biswas, P. 2-D variably-saturated flow: Physical scaling and Bayesian estimation. *J. Hydrol. Eng.* **3**, 223–231 (1998).
- Boufadel, M. C., Suidan, M. T. & Venosa, A. D. A numerical model for density- and viscosity-dependent flows in two-dimensional variably-saturated porous media. *J. Contaminant Hydrol.* **36**, 1–20 (1999).
- Boufadel, M. C. A mechanistic study of nonlinear solute transport in a groundwater-surface water system under steady state and transient hydraulic conditions. *Water Resour. Res.* **36**, 2549–2565 (2000).
- Li, H. L., Zhao, Q. H., Boufadel, M. C. & Venosa, A. D. A universal nutrient application strategy for the bioremediation of oil polluted beaches. *Mar. Pollut. Bull.* **54**, 1146–1161 (2007).
- van Genuchten, M. T. A closed-form equation for predicting the hydraulic conductivity of unsaturated soils. *Soil Sci. Soc. Am. J.* **44**, 892–898 (1980).
- Melchior, P. in *Research in Geophysics* (ed. Odishaw, H.) 183–193 (Massachusetts Institute of Technology Press, 1964).
- Bear, J. *Dynamics of Fluids in Porous Media* (American Elsevier, 1972).
- Zheng, C. & Bennett, G. D. *Applied Contaminant Transport Modelling* 2nd edn (Wiley, 2002).

## Acknowledgements

This work was supported by the Exxon Valdez Oil Spill Trustee Council (No. 070836). However, it does not necessarily reflect the views of the Council, and no official endorsement should be inferred. H.L. thanks the 111 Project (B08030) and the Tianjin Coastal Geology & Environment Survey Project (No. 1212010814005) for partial support. Suggestions from J. Michel on the geomorphology of the beaches are appreciated. We thank many Temple University faculty and students who assisted in this work.

## Author contributions

All authors contributed equally to this work.

## Additional information

The authors declare no competing financial interests. Supplementary information accompanies this paper on [www.nature.com/naturegeoscience](http://www.nature.com/naturegeoscience). Reprints and permissions information is available online at <http://npg.nature.com/reprintsandpermissions>. Correspondence and requests for materials should be addressed to M.C.B.